IEEE Access
Multidisciplinary | Rapid Review | Open Access Journal

Received December 8, 2021, accepted January 11, 2022, date of publication January 14, 2022, date of current version January 21, 2022.

Digital Object Identifier 10.1109/ACCESS.2022.3143582

Attenuation of Microwave Radiation by Post-Anode Plasma in a Composite Grid Electrode Structure

XINGBAO LYU[1], CHENGXUN YUAN[1,2], SVETLANA AVTAEVA[1,2,3], (Member, IEEE), ANATOLY KUDRYAVTSEV[1,2,4], JINGFENG YAO[1], YANGGUO LIU[1], ZHONGXIANG ZHOU[1,2], AND XIAOOU WANG[1]

[1]School of Physics, Harbin Institute of Technology, Harbin 150001, China
[2]Heilongjiang Provincial Key Laboratory of Plasma Physics and Application Technology, Harbin 150001, China
[3]Institute of Laser Physics SB RAS, 630090 Novosibirsk, Russia
[4]Physics Department, St. Petersburg State University, 198504 St. Petersburg, Russia

Corresponding author: Chengxun Yuan (yuancx@hit.edu.cn)

This work was supported by the National Natural Science Foundation of China (NSFC) under Grant 12175050 and Grant 11775062.

ABSTRACT This paper presents a new composite grid electrode structure for the generation of plasma that is suitable for modeling microwave radiation transmission through atmospheric plasma. The new grid anode-composite cathode (GA-CC) structure is to be contrasted with the ordinary grid anode-cathode plate (GA-CP) structure. It is found that the breakdown voltage of the new GA-CC electrode structure is lower than that of the GA-CP structure and is a bit shifted to the right on the *Pd*-axis. An advantage of the GA-CC structure over the GA-CP structure is that it requires a lower voltage to generate the same current. It is found that plasma generated by the new GA-CC structure selectively strengthens electromagnetic waves attenuation in the frequency range of 9-12 GHz.

INDEX TERMS Grid anode, composite cathode, microwave attenuation, Paschen curves, current-voltage characteristics.

I. INTRODUCTION

The propagation of electromagnetic waves in plasma is attracting increased interest among researchers [1]–[5]. Global communication is becoming ever more important, and that communicating depends on the transmission of electromagnetic waves through the atmosphere, much of it through ionosphere, where plasma is the atmosphere's basic state. Plasma absorbs electromagnetic energy, weakening signals and distorting the transmitted information. It is therefore important to study the transmission of electromagnetic waves through the atmospheric plasma layer.

In studying electromagnetic wave transmission in lower atmospheric layers, there are two main plasma-related problems to be addressed. One is ''stealth'' technology [6]–[14]. The other is the blackout (or black barrier) phenomenon [15]–[22]. Plasma stealth technology is the formation of a plasma layer on the surface of a target, making the target more difficult to detect. The use of a plasma as a stealth medium has two advantages: (1) It avoids the loss of aerodynamic shape in the design of a stealth or low-visibility, aircraft. (2) The plasma can be designed to have wide absorption bands with high electromagnetic absorption capability [23]. The black barrier phenomenon is also a problem in the field of aviation. Friction between the aircraft's surface and the atmosphere creates plasma as the aircraft flies at high speed through the atmosphere. The existence of this layer of plasma leads to a communication barrier between the ground and the aircraft. In extreme cases, communication may even be interrupted.

In order to deal with these problems, it is important to study the interaction mechanism of plasma and electromagnetic waves, a topic that has attracted much recent attention. X. Y. Chen *et al.* studied an ultra-wideband absorber structure based on plasma stability. In this paper we propose that the inhomogeneous distribution of the plasma is a key to obtaining ultra-wideband wave absorption. Then we analyze the electromagnetic reflection and absorption situation using the scattering matrix method [23]. W. Y. Zhang *et al.* analyzed the interaction of electromagnetic waves with plasma

The associate editor coordinating the review of this manuscript and approving it for publication was Yi Ren.

through numerical simulations. Wave attenuation in plasma is characterized by band attenuation. The electromagnetic radiation decay improves significantly with a monotonic increase in gas pressure and plasma thickness. As power increases, the wave-decay band width and amplitude increase [24]. J. Zhang *et al.* investigated the effect of the dust size distribution on the transport of electromagnetic waves in a weakly ionized dust plasma. They found that the attenuation of electromagnetic waves is mainly determined by the largest dust particles. The larger the dust particles, the stronger the decay of the electromagnetic waves [25]. Z. Y. Wang *et al.* studied the phase-shift properties of electromagnetic waves in the plasma and the interaction of phase shift with the plasma electron density, collision frequency, and incident frequency [26].

Our laboratory has designed a new device that provides a planar plasma source. Our design idea comes from analysis of some prior research. A promising method of producing plasma that is able to provide the ''stealth'' effect is plasma generation by high-energy electron beams (tens to hundreds of keV), which have high ionizing ability. In recent decades a number of publications reported on the generation of electron beams in glow discharges with a grid electrode. J. J. Rocca *et al.* studied glow discharge's working characteristics using a grid anode structure to produce an electron beam and compared the electron-beam formed by ten different cathode materials. The efficiency of electron beam generation can reach 50-80% by ion bombardment of cathode materials with a high secondary electron emission coefficient [27]. P. A. Bokhan *et al.* designed a discharge structure with self-sustaining photoelectric discharge. In this discharge structure, the anode adopts an open-hole structure. A mechanism for the high efficiency of electron beam generation has been proposed [28]. A. I. Golovin studied the electron beam generation process based on a grid anode open discharge and obtained its discharge current and voltage characteristics [29]. R. L. Gao and J. S. Jia studied large-area plasma characteristics produced by glow discharge with a coaxial grid hollow cathode [30]–[32]. S. G. Belostotsky *et al.* proposed a method to measure the luminous efficiency of the cathode phosphor's coating by using the electron beam generated by gas discharge with a grid electrode [33]. A deeper understanding of the grid discharge structure is gradually developing, and now such structures can be used to generate large areas of planar plasma suitable for attenuation of electromagnetic waves.

It is essential to study the propagation characteristics of electromagnetic waves in plasma of large plane area. We therefore developed a large-area device, and use it to study the characteristics of plasmas. The main focus of this research was to study characteristics of plasmas generated in the post-anode space of grid glow discharges [34]–[38]. Other methods for studying large-area plasmas have also been developed [39]–[42].

There have also been some studies of glow discharges with brush and reverse-brush electrodes. K. Persson studied a plasma generator with a brush electrode and found that the brush electrode's plasma had a high electron density. The electron density in helium plasma was 10^{10}-10^{14} cm^{-3}, and the electron temperature was in the range of 0.05 to 0.10 eV. The brush electrode structure provides a new way to create a plasma layer over a large area with high density [43]. H. M. Musal studied the properties of plasma generated by a plasma source with a reverse-brush electrode structure, and found that the reverse brush electrode structure produces a higher current than the brush electrode structure. The reverse-brush electrode increases the surface area that is generating electrons, which is beneficial for increasing the electron density of the generated plasma [44].

Based on the above research, we first used a conventional DC grid structure that generates the post-anode plasma to carry out experiments with a large area of planar plasma. Because the characteristics of this plasma did not meet the desired parameters, we combined ideas from multiple papers and developed a composite grid electrode structure. This paper presents experimental results of studying characteristics of large-area planar plasmas generated with our new electrode structure and a conventional DC grid structure. We also explore whether the plasma produced by this structure is conducive to the attenuation of electromagnetic waves.

II. EXPERIMENTAL SETUP

In this paper, we report our study of the attenuation of electromagnetic wave transmission by a post-anode plasma, using the arch antenna method, which is based on measuring the attenuation of electromagnetic wave transmission using a Keysight Vector Network Analyzer. The experimental data obtained with this Keysight Vector Network Analyzer were processed to characterize the transmission of plasma generated by a new discharge device with an electrode structure consisting of a grid anode and a composite cathode.

A diagram of the experimental setup is shown in Figure 1. It includes a plasma generating device (3), receiving and transmitting horn antennas (11, 12) and the Keysight Vector Network Analyzer (1), which was used to measure electromagnetic waves attenuation after the wave passes through the plasma. The experimental setup was enclosed with an absorbent sponge (2) to remove interference from the surrounding environment. The plasma-generating device is an electrode structure placed into a discharge chamber made from a dielectric material. The dielectric material used in the cavity is polytetrafluoroethylene. A high-voltage power supply (6) supported a voltage range of 0-2500 V and a current range of 0-10 A, providing power to the discharge. The discharge chamber was pumped by a rotor pump and then filled with helium, whose flow rate was controlled with a trim valve (9). The top wall of the discharge chamber (10) was made from tempered glass that allowed electromagnetic waves to freely penetrate into the discharge chamber as well as enabling observation of the discharge radiation. The surface of the glass wall was placed normal to the path of the incident electromagnetic waves.

The design of an ordinary grid electrode structure is shown in Figure 2. Dimensions of the cathode plate and the grid

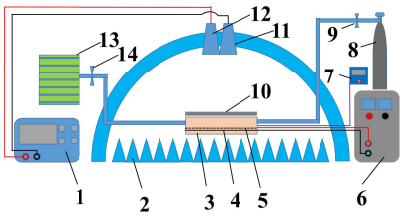

FIGURE 1. A diagram of the experimental setup for measuring plasma attenuation of microwave radiation. 1 - network analyzer, 2 - an absorbent sponge, 3 - plasma generating device, 4 – cathode, 5 – anode, 6 - power supply, 7 - vacuum gauge, 8 - helium tank, 9 - trim valve, 10 - observation window, 11, 12 - receiving and transmitting horn antennas, 13 - vacuum pump, 14 - trim valve.

anode are the same (175 mm × 175 mm). The cathode plate (CP) is made of pure iron with a thickness of 1 mm. The grid anode (GA) is made of stainless steel 304, also with a thickness of 1 mm and with 100 15 mm × 15 mm square holes in a 10 × 10 array. The space between the square holes was 2 mm. Hereinafter, we will refer to this electrode structure as the grid anode-cathode plate (GA-CP) structure.

For the frequency range we used, 8 to 14 GHz, the wavelength range was 3.75 to 2.14 cm. During the measurement process, all possible metal obstacles to transmission were covered with an absorbing sponge. The main area in the cavity where the plasma was formed was much larger than the greatest wavelength of the electromagnetic waves. A vertically incident electromagnetic wave passes through the central regions of the plasma. The density in the domain near the center of the post-anode plasma was uniformly distributed in the transverse direction.

A study of the GA-CP structure showed that the electron density in the post-anode plasma and the degree of helium ionization decrease with increasing helium pressure and increase with increasing discharge current. The electron density in the post-anode plasma is not high: n_e is about $2 \times 10^9 - 6 \times 10^{10}$ cm^{-3}, corresponding to a degree of ionization of about 10^{-7}-10^{-6}. The maximum attenuation of 10-GHz microwave radiation is about 6% at a helium pressure of 2 Torr [45]. The electrode structure shown in Figure 2 has a very low degree of ionization, and the electron density of the generated plasma has a very little influence on the electromagnetic wave transmission.

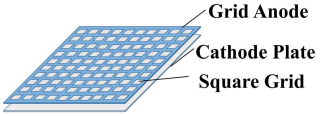

FIGURE 2. The GA-CP structure: grid anode and cathode plate (the GA-CP structure).

We therefore developed a new structure with a grid anode (GA) and a composite cathode (CC). The design of this electrode structure is shown in Figure 3. The electrode sizes of the new structure are the same as the electrode sizes of the GA-CP structure. The grid anode design was the same as in the GA-CP structure (1-mm thick stainless steel plate with 100 15 mm × 15 mm square holes in a 10 × 10 array). The cathode was enhanced with 36 cathode columns arranged on the periphery of the cathode plate. The cathode columns were made of iron and had a diameter of 4 mm and a length of 50 mm. In order to fix the cathode column, the thickness of the cathode plate was increased to 5 mm. A schematic diagram of a cell with a cathode column is shown in Figure 3(b). Hereinafter, we will refer to this electrode structure as the grid anode-composite cathode (GA-CC) structure.

To get the most accurate comparison of the performances of these two electrode structures, we used helium as the working gas. After pumping the cavity to a pressure of 30 Pa, we filled it with helium to reach atmospheric pressure for 2 minutes, and then adjusted it to the pressure required for the experiment. We did not use air as the experimental gas because water vapor present in the ambient air affects the breakdown voltage [46] and the current-voltage characteristics [47], [48]. It should be note that the ambient air temperature in our laboratory was 18-23 °C, and air relative humidity was approximately 10%. At these conditions the water vapor content in helium in the discharge cavity was low and had little impact on the experimental results. We therefore ignored the air influence on characteristics of the discharges.

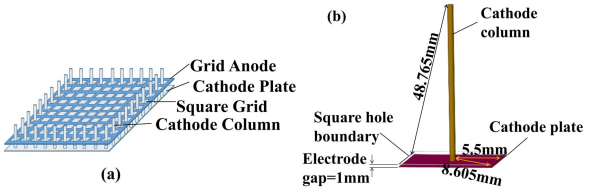

FIGURE 3. (a) The GA-CC structure: grid anode and composite cathode (GA-CC) structure; (b) A schematic diagram of a cell with a cathode column.

III. EXPERIMENTAL RESULTS AND DISCUSSION

Paschen curves and current-voltage characteristics of discharges in these electrode structures as well as attenuation of microwave radiation by a post-anode plasma generated in these two electrode structures, were studied for different lengths of the electrode gap. In order to find out which structure, GA-CP or GA-CC, is more promising, we first measured and compared the Paschen curves and volt-ampere characteristics of these two structures for a helium pressure of 2 Torr.

To measure the Paschen curves for different structures, we used the electrical circuit shown in Figure 2 in ref [49]. The digital oscilloscope was used to measure the breakdown voltage. Stable voltage is displayed by the oscilloscope before and after the breakdown. When the voltage reached the breakdown voltage, the voltage across the discharge gap sharply decreased from the breakdown voltage to the current-limited discharge voltage. At this time, the voltage displayed by the power supply was the breakdown voltage. To reduce errors, the breakdown voltage was averaged after a series of repeated measurements. The error value of the breakdown voltage is approximately $\pm 5V$. After measuring the breakdown voltage U_{br} under certain conditions, the voltage was further applied, and then the voltage of the high-voltage power supply and the

voltage on the resistor were recorded. The voltage U_p across the plasma and the current I in the entire circuit were then determined by these values [49]. To determine the voltage drop U_p on the plasma we are subtracted the voltage drop U_R on the shunt resistor from the output voltage U of the high voltage power supply: $U_p = U - U_R$. The current I of the whole circuit is determined by the voltage U_R and the values of the resistance R: $I = U_R/R$. Throughout the experiment, the surface of the electrode was carefully and regularly cleaned; therefore, the effect of surface impurities was not taken into account, and only the effects of the pressure and electrode gap on the breakdown voltage were considered.

The Paschen curves and current-voltage characteristics of the studied electrode structures are shown in Figures 4 and 5. Figures. 4(a) and 5(a) indicates that the Paschen curves for the composite electrode structure (the GA-CC structure) are a bit shifted to the right along the Pd-axis and downward along the U_{br}-axis compared with these of the GA-CP structure. These differences are greater for a greater gap length between the electrodes. One can see from Figure 5(a) that the breakdown voltage of the new GA-CC structure is significantly lower than that of the ordinary GA-CP structure. However, the difference between the Paschen curves of the two electrode structures completely disappears when the gap length between the electrodes is as small as 1 mm.

Figures. 4(b) and 5(b) show that the voltage values at which the GA-CC electrode structure achieves the same current as the GA-CP electrode structure are lower which can be considered as an advantage of GA-CC. We conclude that the GA-CC electrode structure has an advantage over the ordinary GA-CP electrode structure at all studied electrode gap lengths above 1 mm and for all studied discharge conditions. Measurements of I-V characteristics of the two structures were performed only at voltage below 360 V because we tried to minimize the measurements at great voltages to avoid warming the shunt resistor. These measurements are mainly to compare which structure needs a lower voltage value to achieve the same current value. The measured I-V characteristics indicate that GA-CC has advantage by this criterion.

It should be noted that columns of the composite grid cathode affect the discharge characteristics. This influence can be understood from Figure 3(b). After the cathode columns are added to the cathode plate, the anode and cathode's gap length becomes a range of values rather than a single value. The distance between the electrodes of the GA-CC structure defines the distance between the grid anode and the cathode plate as well as the distance between cathode columns and the grid anode. For example, for the GA-CC structure the cathode-to-anode gap range is from 1 mm up to 5.5-48.765 mm (the error between the dimension measurement of the cathode column and the side length of the square hole is 0.02 mm) when the grid anode and cathode plate's gap is 1 mm (see Figure 3(b)). When the electrode gap length is less than 5.5 mm and Pd is on the right branch of the Paschen curve, the electrode gap's breakdown voltage is determined primarily by gap length between grid anode and cathode plate. However, when the gap length between grid anode and cathode plate is larger than 5.5 mm, the electrode structure's breakdown voltage will be affected by the minimum breakdown path, which is the distance between cathode columns and the grid anode (for gap lengths of 6 and 8 mm). For gap lengths between the grid anode and cathode plate of 6 and 8 mm, the GA-CC structure's breakdown voltage is significantly lower than that of the GA-CP structure (Fig. 5(a)).

It is important to note that there are a number of factors affecting the value of the breakdown voltage of the electrode structure: (1) the product of pressure and the gap length between grid anode and cathode plate [39]; (2) the selection of an optimal breakdown path of the electrode structure by discharge [50]–[53]; (3) variation of the mean free path of electrons between grid anode and cathode plate; (4) change in the energy of electrons [49]; and others. When the pressure increases, the particle density increases and the frequency of electron collisions with neutral particles increases, resulting in more collisions within the electrode gap. The mean free path of the electrons becomes shorter and their energy decreases. This reduces the chance of electrons reaching the anode surface, thereby increasing the breakdown voltage between the grid anode and the cathode.

So, in case if the electrode gap between grid anode and cathode plate is greater than 5.5 mm or Pd value is on the left branch of the Paschen curve, the GA-CC structure has advantages relative to the GA-CP structure. The GA-CC structure can generate a higher current under lower voltage. This advantage should lead to producing plasma of higher density behind the anode for a lower voltage. Therefore, it should be expected that the post-anode plasma generated in the GA-CC structure will more strongly attenuate electromagnetic waves. To test this deduction, we measured the attenuation of microwave radiation by both electrode structures.

As can be seen from Figure 4 and 5, the GA-CC structure is more promising for generation of dense post-anode plasma. However, our purpose was to study the characteristics of the plasma at higher pressure, so we chose helium pressure in the range of 5 - 20 Torr for further research.

In order to better compare the difference of microwave attenuation by the two structures, we adopted two approaches: (1) We fixed Pd value and measured attenuation of the microwave radiation by the two structures at various voltage applied to the structures (Figures 6(a), (c), and (e)). (2) We fixed the voltage applied to the structures and obtained attenuation of the microwave radiation at various Pd values (Figures 6(b), (d), and (f)). Using the Vector Network Analyzer we measured the microwave attenuation at 151 points in the 8-14 GHz frequency range (effects of empty structures and environment were removed at the microwave attenuation measurements). The measurements were carried out for a grid anode-cathode plate gap of 1 mm [Figures 6(a) and (b)], 3 mm [Figures 6(c) and (d)], and 5 mm [Figures 6(e) and (f)].

One can see in Figure 6 that post-anode plasmas in the GA-CP structures at helium pressures of 5-10 Torr do not

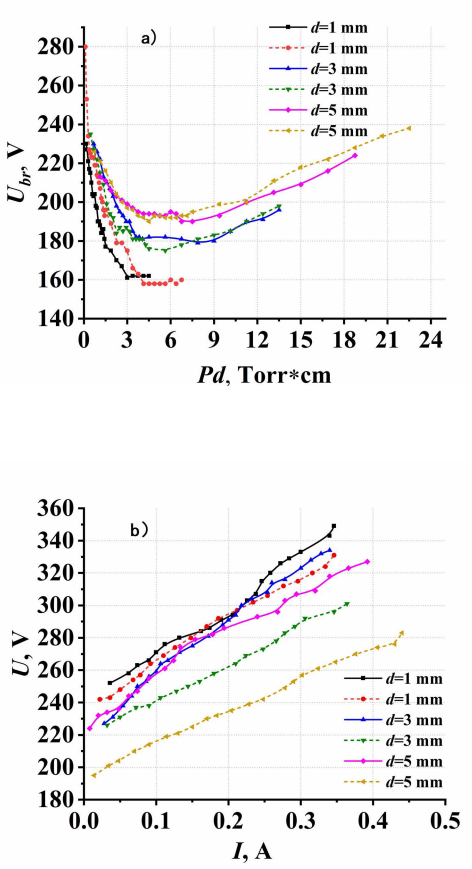

FIGURE 4. (a) The Paschen curves and (b) the current-voltage characteristics of the two electrode structures for electrode gap lengths of 1-5 mm. Solid curves, GA-CP; dashed curves, GA-CC. The current-voltage characteristics were obtained at a helium pressure of 2 Torr.

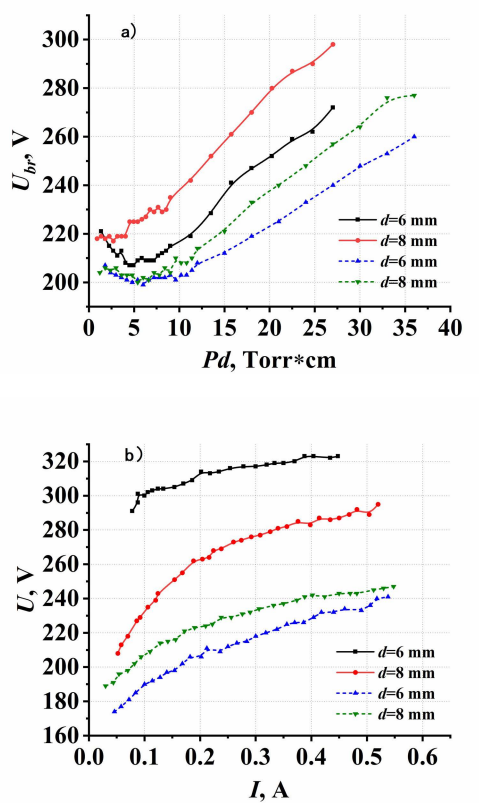

FIGURE 5. (a) The Paschen curves and (b) the current-voltage characteristics of the two electrode structures for electrode gap lengths of 6- and 8-mm. Solid curves, GA-CP; dashed curves, GA-CC. The current-voltage characteristics were obtained at a helium pressure of 2 Torr.

attenuate the microwave radiation, that small attenuation is observed at a pressure of 15 Torr and electrode gap of 3mm, and that maximum attenuation occurs at a frequency near 10.5 GHz. Simultaneously, there is significant attenuation of the microwave radiation (up to 10%) with maximum attenuation in the frequency region near 10.5-11 GHz by the post-anode plasma of the GA-CC structure. For the same GA-CC structure (at unchanged gap length) the attenuation of the microwave radiation by the post-anode plasma increases with increasing applied voltage between the anode and cathode and decreases with increasing helium pressure, except for the GA-CC structure with an electrode gap length of 1 mm, for which the pressure dependence of the attenuation is non-monotonic.

In Figure 6, it can be seen that some attenuation values of electromagnetic wave for plasma in the post-anode space of the GA-CP are positive. We believe that the negative conductivity of the plasma space behind the anode in some frequency ranges may result in an electromagnetic wave gain rather than attenuation [54], [55].

Figure 7 presents the effect of the electrode gap's length on the attenuation of microwave radiation in the post-anode plasma of the GA-CC structure for a fixed voltage and pressures of 5 Torr and 10 Torr. One can see that attenuation of the microwave radiation is largest when the gap length between the grid anode and the cathode plate is 1 mm, and attenuation is least for a gap length of 3 mm. Attenuation for the gap length of 5 mm is occupies an intermediate. There is therefore an optimal value of the electrode gap length at which the relaxation length of the electron energy is greater than that of the electrode gap, and the energy loss of fast electrons in the electrode gap is minimized. As plasma density increases, the number of fast electrons entering the post-anode space is increased, and the density of the post-anode space's plasma is increased. Also, when the electrode gap is greater than or close to the electron energy relaxation length, the discharge current is greater for an electrode gap of 3 mm or 5 mm than for a gap of 1 mm, as shown in Figure 4. At the same time, the decay of the electromagnetic waves in the post-anode plasma of the discharge with an electrode gap of 3 mm and 5 mm is less than that with a 1-mm electrode gap.

To estimate the electron number density we use the microwave phase shift method [45]. We find that when the electrode gap length is 1-5 mm, the average electron number density in the post-anode space varies within the range of 1.3×10^{10} cm^{-3} to 7×10^{10} cm^{-3} at a discharge voltage of 500 V and helium pressures of 5-15 Torr [45]. Corresponding plasma frequencies, $f_{pe} = \omega_{pe}/2\pi \approx 8980\sqrt{n_e}$, are in the range of 1.2-2.4 GHz. Here, n_e is the electron number density

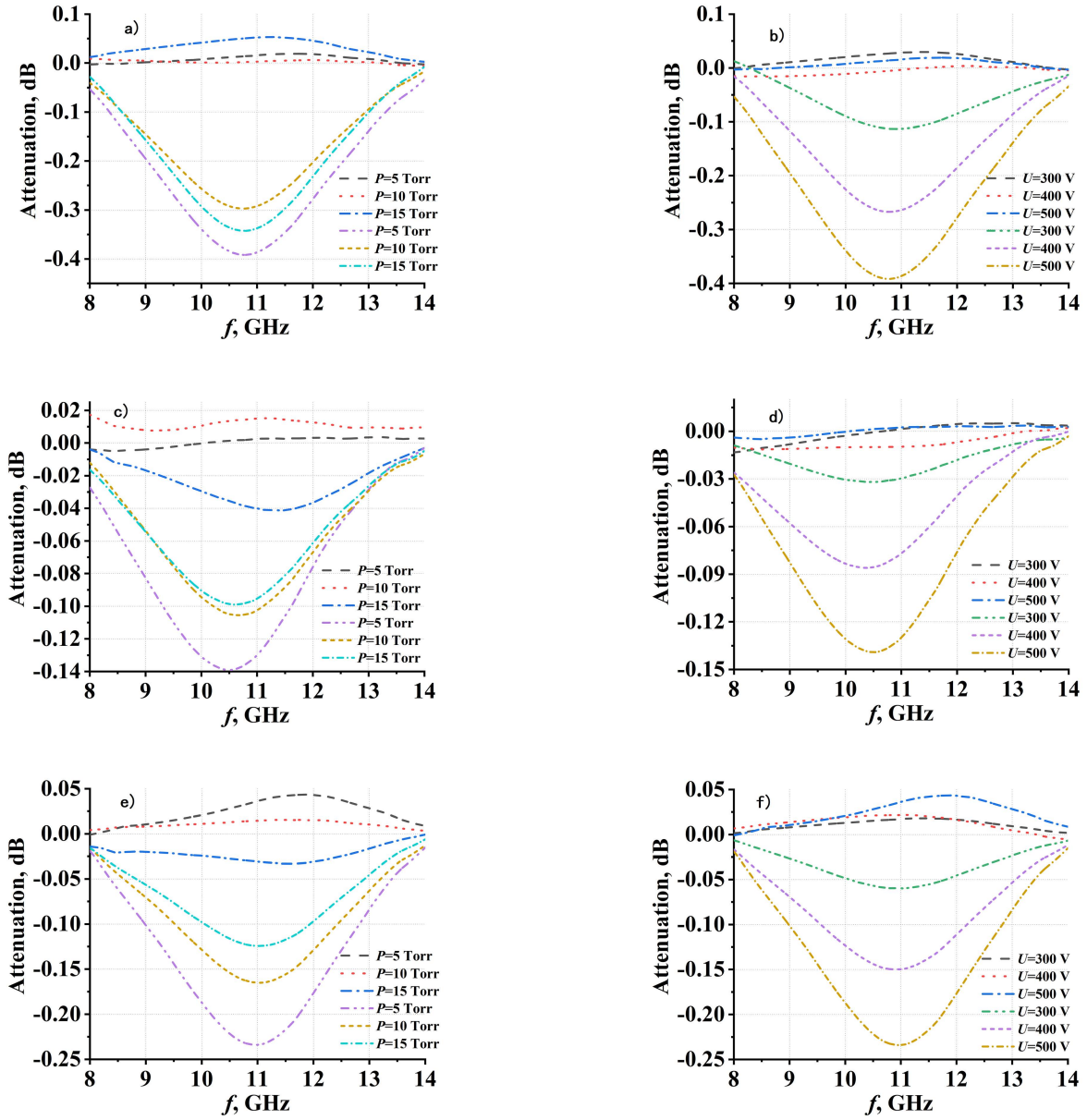

FIGURE 6. Attenuation of microwave radiation by the post-anode plasma of the GA-CP and GA-CC structures with different lengths of the electrode gap: (a, b) 1 mm; (c, d) 3 mm; and (e, f) 5 mm. Dash curve, Dot curve, Dash dot curve: GA-CP; Dash dot dot curve, Short dash curve, Short dash dot curve: GA-CC. For graphs (a), (c), and (e), U = 500 V. For graphs (b), (d), and (f), P = 5 Torr.

in cm^{-3}, $\omega_{pe} = \left(e^2 n_e / m\varepsilon_0\right)^{1/2}$, m and e are, respectively, the mass and charge of an electron, and ε_0 is the permittivity of free space.

As it was shown above, for gap lengths between the grid anode and cathode plate of 6 and 8 mm, the GA-CC structure's breakdown voltage is significantly lower than that of the GA-CP structure. At these gap lengths, we observed the largest deviations between *I-V* characteristics of the GA-CC and GA-CP configurations. Therefore, we measured microwave attenuation for these structures with the electrode gap of 6 mm. The results of the measurements are shown in Figure 8. Comparing these attenuation curves with those on Figs. 6 e,f (for 5 mm gap length) one can note that there is no essential difference between attenuation curves of the GA-CC and GA-CP structures with gap lengths 5 and 6 mm. We believe that this due to a decrease in the energy of runaway electrons with an increase in the electrode gap and, hence, a decrease in the electron density in the post-anode plasma.

The study showed the GA-CC structure is more promising for the generation of dense post-anode plasma. We suppose that advantage of the GA-CC structure over the GA-CP structure is due to the additional acceleration of runaway electrons and the secondary electrons generated by them in the post-anode space in the electric field produced by

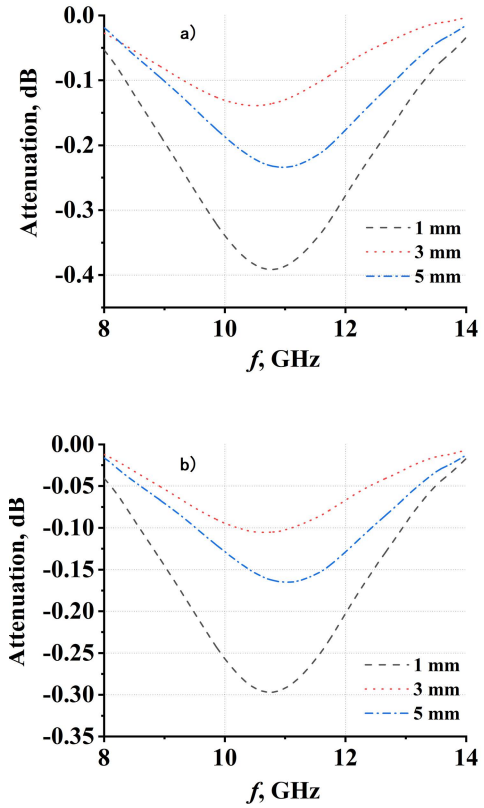

FIGURE 7. Attenuation of the microwave radiation in the GA-CC structure with electrode gap lengths of 1-5 mm at a glow discharge voltage of 500 V, for pressure of (a) 5 Torr and (b) 10 Torr.

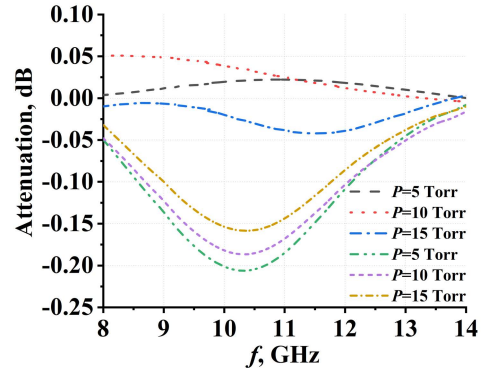

FIGURE 8. Attenuation of the microwave radiation in the GA-CP structure and the GA-CC structure with electrode gap lengths of 6 mm at a glow discharge voltage of 500 V, for pressure of 5 Torr, 10 Torr and 15 Torr. Dash curve, Dot curve, Dash dot curve: GA-CP; Dash dot dot curve, Short dash curve, Short dash dot curve: GA-CC.

cathode columns. Therefore, electron energy and, consequently, their number density in post-anode plasma is higher for GA-CC structure which explains the increase in the attenuation of microwave radiation in the post-anode plasma of this structure.

IV. CONCLUSION

We designed a new composite grid electrode structure (GA-CC) for the generation of plasma that is suitable for modeling microwave radiation transmission through atmospheric plasma. Its characteristics were studied and compared with those of an ordinary grid electrode structure (GA-CP). It was found that the breakdown voltage of the GA-CC electrode structure is lower than that of the GA-CP structure and a bit shifted to the right on the *Pd*-axis. A study of current-voltage characteristics shows that a lower voltage needs for the GA-CC structure compared with the GA-CP structure to generate the same current. This advantage leads to the production of higher-density plasma behind the anode for lower voltage.

In the post-anode plasma of the GA-CP structures, small attenuation of microwaves was observed only at a helium pressure of 15 Torr. But with the GA-CC structure, attenuation of the microwave radiation up to ∼10% (−0.4 dB), with a maximum attenuation in the frequency region near 10.5-11 GHz, was obtained in the post-anode plasma. These experimental results show that the electron density of the plasma generated by the new electrode structure is not high enough to provide strong absorption of the microwave radiation for frequencies of 8-14 GHz. But the attenuation of microwave radiation by the GA-CC structure is much higher than that by the GA-CP structure. For frequencies of 10.5-11 GHz, attenuation reaches 10% for the GA-CC structure with a gap distance of 1 mm. This indicates that a small gap length between grid anode and cathode plate in combination with increased electric field in post-anode space leads to more intense ionization in the post-anode space, which results in greater plasma density and as a consequence, a greater attenuation of microwave radiation. In addition, we found that this new electrode structure can selectively enhance the absorption of an electromagnetic wave in the frequency range of 9-12 GHz. It can be expected that the density of the post-anode plasma will increase significantly if each cell of the grid anode is provided with a cathode column of smaller diameter so that the transparency of the anode grid changes little as the field in the post-anode space increases. We believe that this design can provide the plasma density needed to significantly attenuate microwave radiation.

REFERENCES

[1] C. Cong, C. Yun-Yun, and C. Fen-Ping, "A comparative study on the propagation characteristics of electromagnetic waves in inhomogeneous plasma sheath," *Optik*, vol. 155, pp. 390–398, Feb. 2018.

[2] R. J. Vidmar, "On the use of atmospheric pressure plasmas as electromagnetic reflectors and absorbers," *IEEE Trans. Plasma Sci.*, vol. 18, no. 4, pp. 733–741, Aug. 1990.

[3] M. Bonitz, N. Horing, and P. Ludwig, *Introduction to Complex Plasmas*. Berlin, Germany: Springer, 2010.

[4] N. den Harder, D. C. M. van den Bekerom, R. S. Al, M. F. Graswinckel, J. M. Palomares, F. J. J. Peeters, S. Ponduri, T. Minea, W. A. Bongers, M. C. M. van de Sanden, and G. J. van Rooij, "Homogeneous CO_2 conversion by microwave plasma: Wave propagation and diagnostics," *Plasma Processes Polym.*, vol. 14, no. 6, Jun. 2017, Art. no. 1600120.

[5] J. H. Zhang, Y. M. Liu, X. P. Li, L. Shi, M. Yang, and B. W. Bai, "2D simulation of the electromagnetic wave across the non-uniform reentry plasma sheath with COMSOL," *AIP Adv.*, vol. 9, no. 5, May 2019, Art. no. 055316.

[6] L. Guo, L. Guo, and J. Li, "Propagation of terahertz electromagnetic waves in a magnetized plasma with inhomogeneous electron density and collision frequency," *Phys. Plasmas*, vol. 24, no. 2, Feb. 2017, Art. no. 022108.
[7] Z. B. Wang, Q. Y. Nie, B. W. Li, and F. R. Kong, "Modeling and simulations on the propagation characteristics of electromagnetic waves in sub-atmospheric pressure plasma slab," *Phys. Plasmas*, vol. 24, no. 1, Jan. 2017, Art. no. 013511.
[8] W. Chen, L.-X. Guo, J.-T. Li, and D. Liu, "Analysis of the electromagnetic wave scattering characteristics of time-varying plasma sheath," in *Proc. IEEE Int. Conf. Comput. Electromagn. (ICCEM)*, Feb. 2016, pp. 40–42.
[9] H. Zhou, X. Li, K. Xie, Y. Liu, B. Yao, and W. Ai, "Characteristics of electromagnetic wave propagation in time-varying magnetized plasma in magnetic window region of reentry blackout mitigation," *AIP Adv.*, vol. 7, no. 2, Feb. 2017, Art. no. 025114.
[10] W. Chen, L. Guo, J. Li, and S. Liu, "Research on the FDTD method of electromagnetic wave scattering characteristics in time-varying and spatially nonuniform plasma sheath," *IEEE Trans. Plasma Sci.*, vol. 44, no. 12, pp. 3235–3242, Dec. 2016.
[11] G. He, Y. Zhan, J. Zhang, and N. Ge, "Characterization of the dynamic effects of the reentry plasma sheath on electromagnetic wave propagation," *IEEE Trans. Plasma Sci.*, vol. 44, no. 3, pp. 232–238, Mar. 2016.
[12] Z. Yang, X. Yin, H. Zhang, and S. Chen, "Analysis of EM wave propagation characteristics in plasma sheath of hypersonic reentry blunted cone," in *Proc. IEEE Int. Conf. Comput. Electromagn. (ICCEM)*, Feb. 2016, pp. 66–68.
[13] W. Song and Z. Hou, "Analysis of electromagnetic wave propagation and scattering characteristics of plasma shealth via high order ADE-ADI FDTD," *J. Electromagn. Waves Appl.*, vol. 30, no. 10, pp. 1321–1333, 2016.
[14] Y. Xin, W. Bing, and W. Qian, "A special transmission characteristic of the electromagnetic wave in the plasma sheath surrounding a near-space vehicle and its analysis," in *Proc. 11th Int. Symp. Antennas, Propag. EM Theory (ISAPE)*, Oct. 2016, pp. 412–414.
[15] B. Chaudhury and S. Chaturvedi, "Three-dimensional computation of reduction in Radar cross section using plasma shielding," *IEEE Trans. Plasma Sci.*, vol. 33, no. 6, pp. 2027–2034, Dec. 2005.
[16] C. X. Yuan, Z. X. Zhou, and H. G. Sun, "Reflection properties of electromagnetic wave in a bounded plasma slab," *IEEE Trans. Plasma Sci.*, vol. 38, no. 12, pp. 3348–3355, Dec. 2010.
[17] C.-X. Yuan, Z.-X. Zhou, J. W. Zhang, X.-L. Xiang, Y. Feng, and H.-G. Sun, "Properties of propagation of electromagnetic wave in a multilayer radar-absorbing structure with plasma- and radar-absorbing material," *IEEE Trans. Plasma Sci.*, vol. 39, no. 9, pp. 1768–1775, Sep. 2011.
[18] B. Bai, X. Li, J. Xu, and Y. Liu, "Reflections of electromagnetic waves obliquely incident on a multilayer stealth structure with plasma and radar absorbing material," *IEEE Trans. Plasma Sci.*, vol. 43, no. 8, pp. 2588–2597, Aug. 2015.
[19] J. Xu, B. Bai, C. Dong, Y. Zhu, Y.-Y. Dong, and G. Zhao, "A novel plasma jamming technology based on the resonance absorption effect," *IEEE Antennas Wireless Propag. Lett.*, vol. 16, pp. 1056–1059, 2017.
[20] J. Xu, B. Bai, C. Dong, Y. Dong, Y. Zhu, and G. Zhao, "Evaluations of plasma stealth effectiveness based on the probability of radar detection," *IEEE Trans. Plasma Sci.*, vol. 45, no. 6, pp. 938–944, Jun. 2017.
[21] B. Bai, X. Li, Y. Liu, J. Xu, L. Shi, and K. Xie, "Effects of reentry plasma sheath on the polarization properties of obliquely incident EM waves," *IEEE Trans. Antennas Propag.*, vol. 42, no. 10, pp. 3365–3372, Oct. 2014.
[22] X. Wei, H. Xu, J. Li, M. Lin, and H. Song, "Comparison study of electromagnetic wave propagation in high and low pressure Ar inductively coupled plasma," *Vacuum*, vol. 127, pp. 65–72, May 2016.
[23] X. Chen, F. Shen, Y. Liu, W. Ai, and X. Li, "Study of plasma-based stable and ultra-wideband electromagnetic wave absorption for stealth application," *Plasma Sci. Technol.*, vol. 20, no. 6, Jun. 2018, Art. no. 065503.
[24] W. Zhang, H. Xu, X. Wei, X. Han, and Z. Song, "Numerical simulation of the interaction between electromagnetic wave and plasma," *IOP Conf. Ser., Mater. Sci. Eng.*, vol. 569, Aug. 2019, Art. no. 022032.
[25] J. Zhang, S. Yan, S. Zhao, G. Zhang, and W. Duan, "The effect of dust size distribution on the propagation of electromagnetic waves in a weakly ionized dusty plasma," *J. Phys., Conf. Ser.*, vol. 1626, no. 1, Oct. 2020, Art. no. 012008.
[26] Z. Wang, L. Guo, and J. Li, "Research on phase shift characteristics of electromagnetic wave in plasma," *Plasma Sci. Technol.*, vol. 23, no. 7, Jul. 2021, Art. no. 075001.
[27] J. J. Rocca, J. D. Meyer, M. R. Farrell, and G. J. Collins, "Glow-discharge-created electron beams: Cathode materials, electron gun designs, and technological applications," *J. Appl. Phys.*, vol. 56, no. 3, pp. 790–797, Aug. 1984.
[28] P. A. Bokhan and D. E. Zakrevsky, "Self-sustained photoelectron discharge," *Appl. Phys. Lett.*, vol. 81, no. 14, pp. 2526–2528, Sep. 2002.
[29] A. I. Golovin, E. K. Egorova, and A. I. Shloido, "Estimation of the current-voltage characteristic of an open discharge," *Tech. Phys.*, vol. 59, no. 10, pp. 1445–1451, Oct. 2014.
[30] R. Gao, C. Yuan, S. Liu, F. Yue, J. Jia, Z. Zhou, J. Wu, and H. Li, "Broadband microwave propagation in a novel large coaxial gridded hollow cathode helium plasma," *Phys. Plasmas*, vol. 23, no. 6, Jun. 2016, Art. no. 063304.
[31] R. Gao, C. Yuan, H. Li, J. Jia, Z.-X. Zhou, J. Wu, Y. Wang, and X. Wang, "Absolute continuum intensity diagnostics of a novel large coaxial gridded hollow cathode argon plasma," *Phys. Plasmas*, vol. 23, no. 8, Aug. 2016, Art. no. 083525.
[32] J. Jia, C. Yuan, A. A. Kudryavtsev, S. I. Eliseev, G. V. Kirsanov, V. S. Bekasov, R. Gao, and Z. Zhou, "Numerical and experimental diagnostics of dusty plasma in a coaxial gridded hollow cathode discharge," *IEEE Trans. Plasma Sci.*, vol. 44, no. 12, pp. 2973–2978, Dec. 2016.
[33] S. G. Belostotsky, D. V. Lopaev, Y. A. Mankelevich, E. A. Muratov, A. T. Rakhimov, V. B. Saenko, and M. A. Timofeev, "Light efficiency of cathodoluminescent screens excited by a runaway electron beam," *Plasma Phys. Rep.*, vol. 34, no. 11, pp. 969–977, Nov. 2008.
[34] J. T. Gudmundsson and A. Hecimovic, "Foundations of DC plasma sources," *Plasma Sources Sci. Technol.*, vol. 26, no. 12, Nov. 2017, Art. no. 123001.
[35] C. Yuan, R. Tian, S. I. Eliseev, V. S. Bekasov, E. A. Bogdanov, A. A. Kudryavtsev, and Z. Zhou, "Numerical simulation and analysis of electromagnetic-wave absorption of a plasma slab created by a direct-current discharge with gridded anode," *J. Appl. Phys.*, vol. 123, no. 11, Mar. 2018, Art. no. 113303.
[36] C. Yuan, J. Yao, S. I. Eliseev, E. A. Bogdanov, A. A. Kudryavtsev, and Z. Zhou, "On self-sustainment of DC discharges with gridded anode," *J. Appl. Phys.*, vol. 122, no. 14, Oct. 2017, Art. no. 143304.
[37] A. A. Kudryavtsev, A. V. Morin, and L. D. Tsendin, "Role of nonlocal ionization in formation of the short glow discharge," *Tech. Phys.*, vol. 53, no. 8, pp. 1029–1040, 2008.
[38] S. I. Eliseev, E. A. Bogdanov, and A. A. Kudryavtsev, "Slow electron energy balance for hybrid models of direct-current glow discharges," *Phys. Plasmas*, vol. 24, no. 9, Sep. 2017, Art. no. 093503.
[39] M. A. Lieberman and A. J. Lichtenberg, *Principles of Plasma Discharges and Materials Processing: Lieberman/Plasma 2e*. Hoboken, NJ, USA: Wiley, 2005.
[40] A. Y. Nikiforov, C. Leys, M. A. Gonzalez, and J. L. Walsh, "Electron density measurement in atmospheric pressure plasma jets: Stark broadening of hydrogenated and non-hydrogenated lines," *Plasma Sources Sci. Technol.*, vol. 24, no. 3, Apr. 2015, Art. no. 034001.
[41] V. I. Demidov, M. E. Koepke, I. P. Kurlyandskaya, and M. A. Malkov, "Feasibility, strategy, methodology, and analysis of probe measurements in plasma under high gas pressure," *J. Phys., Conf. Ser.*, vol. 958, Feb. 2018, Art. no. 012003.
[42] V. I. Demidov, S. V. Ratynskaia, and K. Rypdal, "Electric probes for plasmas: The link between theory and instrument," *Rev. Sci. Instrum.*, vol. 73, no. 10, pp. 3409–3439, Oct. 2002.
[43] K. Persson, "Brush cathode plasma—A well-behaved plasma," *J. Appl. Phys.*, vol. 36, no. 10, pp. 3086–3094, Oct. 1965.
[44] H. M. Musal, "An inverse brush cathode for the negative-glow plasma source," *J. Appl. Phys.*, vol. 37, no. 4, pp. 1935–1937, Mar. 1966.
[45] X. Lyu, C. Yuan, S. Avtaeva, A. Kudryavtsev, J. Yao, Z. Zhou, and X. Wang, "A large-area DC grid anode glow discharge in helium," *Plasma Phys. Rep.*, vol. 47, no. 4, pp. 369–376, Apr. 2021.
[46] E. Kuffel, "Electron attachment coefficients in oxygen, dry air, humid air and water vapour," *Proc. Phys. Soc.*, vol. 74, no. 3, pp. 297–308, Sep. 1959.
[47] B. Li, X. Li, M. Fu, R. Zhuo, and D. Wang, "Effect of humidity on dielectric breakdown properties of air considering ion kinetics," *J. Phys. D, Appl. Phys.*, vol. 51, no. 37, Sep. 2018, Art. no. 375201.
[48] L. Zavattoni, R. Hanna, O. Lesaint, and O. Gallot-Lavallée, "Dark current measurements in humid SF6: Influence of electrode roughness, relative humidity and pressure," *J. Phys. D, Appl. Phys.*, vol. 48, no. 37, Sep. 2015, Art. no. 375501.

[49] X. Lyu, C. Yuan, S. Avtaeva, A. Kudryavtsev, J. Yao, Z. Zhou, and X. Wang, "Paschen curves and current–voltage characteristics of large-area short glow discharge with different electrode structures," *Phys. Plasmas*, vol. 27, no. 12, Dec. 2020, Art. no. 123509.
[50] Y. Fu, P. Zhang, J. P. Verboncoeur, and X. Wang, "Electrical breakdown from macro to micro/nano scales: A tutorial and a review of the state of the art," *Plasma Res. Exp.*, vol. 2, no. 1, Feb. 2020, Art. no. 013001.
[51] Y. Fu, P. Zhang, and J. P. Verboncoeur, "Gas breakdown in atmospheric pressure microgaps with a surface protrusion on the cathode," *Appl. Phys. Lett.*, vol. 112, no. 25, Jun. 2018, Art. no. 254102.
[52] Y. Fu, P. Zhang, and J. P. Verboncoeur, "Paschen's curve in microgaps with an electrode surface protrusion," *Appl. Phys. Lett.*, vol. 113, no. 5, Jul. 2018, Art. no. 054102.
[53] Y. Fu, P. Zhang, J. Krek, and J. P. Verboncoeur, "Gas breakdown and its scaling law in microgaps with multiple concentric cathode protrusions," *Appl. Phys. Lett.*, vol. 114, no. 1, Jan. 2019, Art. no. 014102.
[54] J. Yao, C. Yuan, Z. Yu, I. P. Kurlyandskaya, V. I. Demidov, A. A. Kudryavtsev, T. V. Rudakova, and Z. Zhou, "Nonlocal control of plasma conductivity," *Phys. Plasmas*, vol. 26, no. 7, Jul. 2019, Art. no. 073301.
[55] C. Yuan, J. Yao, E. A. Bogdanov, A. A. Kudryavtsev, and Z. Zhou, "Formation of inverse electron distribution function and absolute negative conductivity in nonlocal plasma of a DC glow discharge," *Phys. Rev. E, Stat. Phys. Plasmas Fluids Relat. Interdiscip. Top.*, vol. 101, no. 3, Mar. 2020, Art. no. 031202.

XINGBAO LYU received the bachelor's degree in physics from Liaocheng University, China, in 2006. He is currently pursuing the Ph.D. degree with the Harbin Institute of Technology, China.

Since 2007, he has been studying at the School of Physics, Harbin Institute of Technology. His research interests include studying the fundamental properties of atmospheric plasma and the interaction between plasma and electromagnetic waves.

CHENGXUN YUAN received the bachelor's and Ph.D. degrees from the Harbin University of Technology, in 2004 and 2011, respectively.

He is currently a Professor with the School of Physics, Harbin Institute of Technology, China. He has more than 100 publications in the plasma field. His research interests include basic plasma physics, dusty plasma physics, and the interaction of electromagnetic radiation with plasma.

SVETLANA AVTAEVA (Member, IEEE) received the Ph.D. degree in physico-mathematical science from Lomonosov's Moscow State University, Russia, in 2012.

Since September 2017, she has been the Senior Scientist with the Laboratory of Super-Short Laser Pulse Physics, Institute of Laser Physics SB RAS, Novosibirsk. She had over 150 papers published in scientific journals, books, and conference proceedings, and one monograph.

ANATOLY KUDRYAVTSEV received the M.S. and Ph.D. degrees in physics from Leningrad State University, Saint Petersburg, Russia, in 1976 and 1983, respectively.

Since 1982, he has been with Saint Petersburg State University, where he is currently an Associate Professor with the Optics Department. He is an Expert in the gas discharge physics and kinetic theory of plasma physics. He is the author of over 100 journal articles and numerous conference presentations.

JINGFENG YAO received the bachelor's and Ph.D. degrees from the Harbin University of Technology, in 2015 and 2020, respectively.

He is currently a Professor with the School of Physics, Harbin Institute of Technology, China. He has more than 30 publications in the plasma field. His research interests include basic plasma physics, dusty plasma physics, and the interaction of electromagnetic radiation with plasma.

YANGGUO LIU received the bachelor's degree in physics from the Shandong University of Technology, China, in 2019. He is currently pursuing the master's degree with the Harbin Institute of Technology, China.

Since 2019, he has been studying at the School of Physics, Harbin Institute of Technology. His research interest includes plasma spectral diagnostics.

ZHONGXIANG ZHOU received the B.S. degree in physics from Jilin University, Changchun, China, in 1987, and the Ph.D. degree in optics from the Harbin Institute of Technology (HIT), Harbin, China, in 1997.

Since 2000, he has been a Full Professor of physics with the Department of Physics, HIT. His research interests include electromagnetic-wave interactions with plasma, dusty plasma, and terahertz technology.

XIAOOU WANG received the B.S. degree in physics from Northeast Normal University, Changchun, China, in 1983, and the Ph.D. degree in optics from the Harbin Institute of Technology (HIT), Harbin, China.

Since 1995, she has been a Full Professor of physics with the Department of Physics, HIT. Her research interests include electromagnetic-wave interactions with plasma, dusty plasma, and terahertz technology.